Molecular Crystals and Liquid Crystals
Publication details, including instructions for authors and subscription information:
http://www.tandfonline.com/loi/gmcl20

Two-Beam Energy Exchange in a Hybrid Photorefractive Inorganic-Cholesteric Cell

V. Yu. Reshetnyak [a], I. P. Pinkevych [a], G. Cook [b c], D. R. Evans [b] & T. J. Sluckin [d]

[a] Physics Faculty, National Taras Shevchenko University of Kyiv, Volodymyrs'ka Street 64, Kyiv, 01601, Ukraine

[b] Air Force Research Laboratory, Materials and Manufacturing Directorate, Wright-Patterson Air Force Base, Ohio, 45433, USA

[c] Universal Technology Corporation, 1270 N. Fairfield Road, Dayton, Ohio, 45432, USA

[d] School of Mathematics, University of Southampton, Highfield, Southampton, SO17 1BJ, United Kingdom

Version of record first published: 15 May 2012.

To cite this article: V. Yu. Reshetnyak , I. P. Pinkevych , G. Cook , D. R. Evans & T. J. Sluckin (2012): Two-Beam Energy Exchange in a Hybrid Photorefractive Inorganic-Cholesteric Cell, Molecular Crystals and Liquid Crystals, 560:1, 8-22

To link to this article: http://dx.doi.org/10.1080/15421406.2012.661950

Mol. Cryst. Liq. Cryst., Vol. 560: pp. 8–22, 2012

ISSN: 1542-1406 print/1563-5287 online
DOI: 10.1080/15421406.2012.661950

Taylor & Francis
Taylor & Francis Group

Two-Beam Energy Exchange in a Hybrid Photorefractive Inorganic-Cholesteric Cell

V. YU. RESHETNYAK,[1] I. P. PINKEVYCH,[1] G. COOK,[2,3]
D. R. EVANS,[2] AND T. J. SLUCKIN[4,*]

[1]Physics Faculty, National Taras Shevchenko University of Kyiv, Volodymyrs'ka Street 64, Kyiv 01601, Ukraine
[2]Air Force Research Laboratory, Materials and Manufacturing Directorate, Wright-Patterson Air Force Base, Ohio 45433, USA
[3]Universal Technology Corporation, 1270 N. Fairfield Road, Dayton, Ohio 45432, USA
[4]School of Mathematics, University of Southampton, Highfield, Southampton SO17 1BJ, United Kingdom

We develop a theoretical model to describe two-beam energy exchange in a hybrid photorefractive inorganic-cholesteric cell. A cholesteric LC cell is placed between two inorganic photorefractive windows. Weak and strong light beams are incident on the LC cell. The interfering light beams induce a periodic space-charge field in the photorefractive windows. This penetrates into the LC, inducing a diffraction grating written on the LC director. The theory calculates the energy gain of the weak beam, as a result of its interaction with the pump beam within the diffraction grating. In the theory, the flexoelectric mechanism for electric field-director coupling is a more important than the LC static dielectric anisotropy coupling. The flexoelectric polarization in the bulk LC follows from the initial director pretilt at the cell substrates and is the main physical mechanism governing the magnitude of the director grating and the two-beam coupling. The LC optics is described in the Bragg regime. Theoretical results for exponential gain coefficients have been compared with experimental results for hybrid cells filled with cholesteric mixtures TL205/CB15 and BL038/CB15. In order to reconcile theory and experiment, we require that (a) the magnitude of the director grating must be cubic rather than linear in the space-charge field, and (b) near the cell surface, nematic ordering must dominate. Within this paradigm, we are able to fit experimental data to theory for both cholesteric mixtures, subject to the use of some fitting parameters.

1. Introduction

In recent years, spectacular advances have been reported in liquid crystal photorefractive (LC) cells. In the simplest systems, negative and positive ions are photogenerated in a LC placed in an external light field. The ions give rise to a space-charge electric field. The field then modulates the nematic director field and hence causes a modulation the tensor refractive index [1–3]. However, a second mechanism relates to hybrid organic-inorganic photorefractives, in which a LC sample is placed between photorefractive or

*Address correspondence to T. J. Sluckin, School of Mathematics, University of Southampton, Highfield, Southampton SO17 1BJ, United Kingdom. E-mail: T.J.Sluckin@soton.ac.uk

photoconducting layers [4–6]. Space charges are photo-generated in these layers, leading to space-charge electric fields. These then penetrate into the adjacent LC, and give rise to director modulation. In both cases beam coupling occurs because of the interaction between the incident light and the induced director modulation. The result is an amplification of one of the beams. In a LC beam-coupling geometry the exponential gain coefficients can reach values more than two orders of magnitude larger than those in solid inorganic photorefractive crystals [7–12].

Early theoretical studies of these systems are due to Tabiryan and Umeton [13], and Jones and Cook [14]. These authors suppose that the beam-coupling mechanism in hybrid organic-inorganic photorefractives is analogous to that in conventional LC cells. In this scenario the coupling between the light-induced space-charge electric field and the LC director is caused by the LC static dielectric anisotropy. This picture predicts that the maximal energy transfer will occur for a grating spacing of the order of the LC cell thickness. However, experimental results for hybrid nematic LC cells show conclusively that this maximum takes place at grating spacing [10–12] which are considerably smaller than the cell thickness.

Recently, however, the present authors have returned to the problem of electric field-director coupling in hybrid nematic LC cells [15]. It turns out that most important factor governing the director deformation is the flexoelectric interaction between the director and the electric field, and that this significantly larger than the LC static dielectric anisotropy coupling. In addition, a nonlinear contribution to the magnitude of the director grating as a function of space-charge electric field is required in order to account for the experimental results [10–12], and in Ref. [15] we have discussed possible mechanisms for this nonlinearity.

In recent experimental work, some of us have extended our study of two-wave energy exchange to hybrid cholesteric LC cells [16]. The cholesteric systems exhibit a significant additional feature which had not been observed in hybrid nematic LC cells. In these systems, the sign of the gain coefficient changes as the grating spacing is increased. The present paper uses the paradigm of our earlier paper [15] in order to address this problem. Specifically, we construct a theory for the optical gain characteristics of hybrid cholesteric LC-inorganic photorefractives, in the case when cholesteric ordering is induced in nematic matrices by introducing chiral impurities.

The paper is organized as follows. In Sec. II we introduce the model of hybrid cholesteric cell in the field of the interfering incident light beams and define the evanescent photorefractive field in the LC cell. In Sec. III we derive equations for the LC director subject to this electric field and solve them. In Sec. IV we discuss light propagation in the LC, starting with expressions for the dielectric tensor, going on to equations for the two coupled light modes and expressions for the exponential gain coefficient in the LC cell. In Sec. V we make comparisons with experimental results, and in Sec. VI present some brief conclusions.

2. Photorefractive Electric Field in Liquid Crystal

The hybrid cell consists of flexoelectric cholesteric LC, placed between two plane-parallel transparent photorefractive layers. The LC is bounded by the planes $z = -L/2$ and $z = L/2$. In addition, the LC in the hybrid cell consists of a nematic matrix which contains impurity chiral molecules. These induce a cholesteric helix in the LC [17].

We note, however, a key difference between the influence of surface director pretilt between nematic and cholesteric phases in planar cells [18]. In a nematic the director angle decreases in the bulk linearly with distance. However, in a cholesteric the decrease is exponential.

Here, however, we are not dealing with a pure cholesteric material, but rather a nematic material with chiral impurities. In a system in which the gradient of the director is uniform, the chiral concentration will also be uniform. From the point of view of cholesteric properties, it is unimportant whether the chirality is caused by a homogeneous material of weakly chiral nematic molecules, or by a weak solution of strongly chiral molecules in a nematic matrix. But, as has been pointed out by a number of authors [19, 20], the linear coupling between the concentration and director twist can under some circumstances lead to molecular segregation in which more strongly twisted regions contain a higher concentration of chiral molecules, and weakly twisted regions contain a lower concentration. Under these circumstances a homogeneous cholesteric and a chiral solution in a nematic matrix will behave differently.

We shall suppose that such a circumstance occurs here. We suggest that it is energetically profitable for chiral molecules to aggregate preferentially in the central part of the cell where the angle of nematic director induced by the director pretilt at the cell surfaces is unimportant. We caricature this segregation by making an *ansatz* that the cholesteric twist is confined to a central region of the cell of width l. By contrast, in the thin layers and near the cell surfaces nematic ordering dominates. At this stage the distance l is to be regarded as a fitting parameter in the theory. The cholesteric-nematic segregation is included in the diagram in Fig. 1. We justify the ansatz *ex post facto* because it leads to agreement with experimental results.

The cell is illuminated by two intersecting coherent light beams $\mathbf{E}_1 = A_1(z)\mathbf{e}_1 \exp(i\mathbf{k}_1\cdot\mathbf{r} - i\omega t)$ and $\mathbf{E}_2 = A_2(z)\mathbf{e}_2 \exp(i\mathbf{k}_2\cdot\mathbf{r} - i\omega t)$. The nonlinear properties of both media require that $A_1(z)$, $A_2(z)$ not be constant, but change as a function of position,

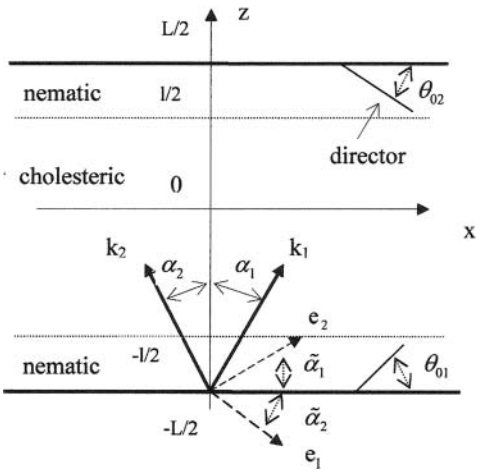

Figure 1. Scheme of the LC cell, showing light beams incident from photorefractive medium, together with associated wave- and polarization vectors. The decomposition of LC into cholesteric and nematic layers, as discussed above, is also shown. Quantities $\mathbf{k}_{1,2}$, $\alpha_{1,2}$, $\tilde{\alpha}_{1,2}$, $\mathbf{e}_{1,2}$, $\theta_{01,2}$ are defined in the text.

as energy exchange takes place between the beams. The bisector of the beams is directed along the z-axis, the wave vectors $\mathbf{k}_1, \mathbf{k}_2$ and the polarization vectors $\mathbf{e}_1, \mathbf{e}_2$ of the beams lie in the xz-plane. The director pretilt at the LC cell boundaries is described respectively by the angles θ_{01}, θ_{02} in the xz-plane. The scheme of the LC cell is shown in Fig. 1.

The beams produce a light intensity interference pattern

$$I(z) = (I_1 + I_2)[1 + \frac{1}{2}(m(z)\exp(iqx) + c.c.)], \tag{1}$$

where we define the modulation parameter $m(z) = 2\cos(2\delta)A_1(z)A_2^*(z)/(I_1 + I_2)$, and where 2δ is the angle between the two incident beams in the photorefractive medium, $I_1 = A_1A_1^*$, $I_2 = A_2A_2^*$ are the intensities of incident beams, and $q = k_{1x} - k_{2x} = 2k\sin\delta \approx 2k\delta$ is the wave number of the intensity pattern. Inside the photorefractive substrates, the light intensity pattern (1) induces a space charge. The space-charge density is modulated along the x-axis with period equal to $2\pi/q$ and gives rise to an electric potential $\tilde{\Phi}(x, z)$

$$\tilde{\Phi}(x, z) = \tilde{\Phi}_0 + [\tilde{\Phi}(z)\exp(iqx) + c.c.], \tag{2}$$

where $\tilde{\Phi}_0$ is an arbitrary constant (which may be taken to be zero), and

$$\tilde{\Phi}(z) = \frac{iE_{sc}(q)}{2q}m(z). \tag{3}$$

In an infinite photorefractive medium and for a diffusion-dominated space-charge field $E_{sc}(q)$ takes the following form [21]:

$$E_{sc}(q) = \frac{iE_d}{1 + \frac{E_d}{E_q}},\ E_d = q\frac{k_bT}{e}, \quad E_q = (1 - \frac{N_a}{N_d})\frac{eN_a}{\varepsilon_0\varepsilon_{Ph}q}, \tag{4}$$

where E_d is the diffusion field, E_q is the so-called saturation field, N_a and N_d are respectively the acceptor and donor impurity densities, ε_{Ph} is the dielectric permittivity of photorefractive material, and e is the electron charge.

The space-charge electric field penetrates into the flexoelectric LC. The electric field obeys the Poisson equation

$$\nabla\cdot(\varepsilon_0\hat{\tilde{\varepsilon}}\cdot\mathbf{E} + \mathbf{P}_f) = 0,\ \mathbf{E} = -\nabla\Phi(x, z), \tag{5}$$

with boundary conditions for $\Phi(x, z)$ created by electric potential (2) at $z = -L/2$ and $z = L/2$. The flexopolarization $\mathbf{P}_f$ is defined by the expression $\mathbf{P}_f = e_1\mathbf{n}\nabla\cdot\mathbf{n} + e_3(\nabla\times\mathbf{n}\times\mathbf{n})$ [17], $\tilde{\varepsilon}_{ij} = \tilde{\varepsilon}_\perp\delta_{ij} + \tilde{\varepsilon}_a n_i n_j$ is the low frequency dielectric permittivity of the LC, n_i are the components of the director **n,** $\tilde{\varepsilon}_a = \tilde{\varepsilon}_| - \tilde{\varepsilon}_\perp$ is the dielectric anisotropy, $\tilde{\varepsilon}_{||}$ and $\tilde{\varepsilon}_\perp$ are the components of the dielectric tensor along and perpendicular to the director**,** e_1 and e_3 are the flexoelectric coefficients.

We solve eq. (5) following the method in our previous paper [15], yielding the following expressions for electric field in LC:

$$\begin{aligned} E_x &= E_{0x}\exp(iqx) + c.c, \\ E_z &= E_{0z}\exp(iqx) + c.c., \end{aligned} \tag{6}$$

$$E_x = -iq\left(\frac{\Phi_1+\Phi_2}{4}\frac{\cosh(\tilde{q}(z)z)}{\cosh(\tilde{q}(z)L/2)}+\frac{\Phi_2-\Phi_1}{4}\frac{\sinh(\tilde{q}(z)z)}{\sinh(\tilde{q}(z)L/2)}\right),$$
$$E_z = -\tilde{q}(z)\left(\frac{\Phi_1+\Phi_2}{4}\frac{\sinh(\tilde{q}(z)z)}{\cosh(\tilde{q}(z)L/2)}+\frac{\Phi_2-\Phi_1}{4}\frac{\cosh(\tilde{q}(z)z)}{\sinh(\tilde{q}(z)L/2)}\right) \quad (7)$$

where $\Phi_1 = \frac{E_{sc}(q)}{q}m(-L/2)$, $\Phi_2 = \frac{E_{sc}(q)}{q}m(L/2)$; $\tilde{q}(z) = q\sqrt{\frac{\tilde{\varepsilon}_{||}}{\tilde{\varepsilon}_\perp}}$ in the nematic layers (i.e. $l/2 < |z| < L/2$) and $\tilde{q}(z) = q\sqrt{\frac{\tilde{\varepsilon}_\perp+\tilde{\varepsilon}_{||}}{2\tilde{\varepsilon}_\perp}}$ in the cholesteric layer (i.e. $|z| < l/2$). Below we shall drop the argument of $\tilde{q}(z)$, and replace it by $\tilde{q}$ where it is possible to do so without ambiguity.

3. LC Director Profile

The equilibrium director profile can be found by minimizing the total free energy functional of the LC cell defined by

$$F = F_{el} + F_l + F_E + F_{fl}, \quad (8)$$

where

$$F_{el} = \frac{1}{2}\int [K_{11}(\nabla\cdot\mathbf{n})^2 + K_{22}(\mathbf{n}\cdot\nabla\times\mathbf{n}+g)^2 + K_{33}(\mathbf{n}\times\nabla\times\mathbf{n})^2]dV,$$
$$F_l = -\frac{\varepsilon_0\varepsilon_a}{4}\int(\mathbf{n}\cdot\mathbf{E}_{hv})^2\,dV, \quad F_E = -\frac{1}{2}\int(\mathbf{D}\cdot\mathbf{E})^2 dV,$$
$$F_{fl} = -\int(\mathbf{P}_f\cdot\mathbf{E})dV, \quad (9)$$

Here F_{el} is the bulk elastic energy of a distorted cholesteric or nematic (if $g = 0$) LC layer; F_l is contribution of the light field to the total free energy functional; F_E is the contribution from the dc-electric field created in the LC cell by the photorefractive layers; F_{fl} is the contribution from interaction of the dc-electric field with the LC flexoelectric polarization; K_{11}, K_{22}, K_{33} are the splay, twist and bend elastic constants respectively; $g = \frac{2\pi}{p_0}$ where p_0 is a pitch of the cholesteric helix; ε_a is the anisotropy of the LC dielectric permittivity at optical frequency; $\mathbf{E}_{hv}$ is the electric vector of the light field in the LC. Finally we suppose infinitely rigid director anchoring at the cell surfaces with the director easy axis along the x-axis.

We now make a number of approximations, first made in our previous paper [15], allowing some terms in eqs. (8,9) to be dropped. We can suppose the LC dielectric anisotropy at optical frequency $\varepsilon_a << 1$, and hence we can neglect the light field contribution F_l to the total free energy. We can also neglect the term F_E which describes the influence of the LC dielectric anisotropy. The net effect is that director reorientation should be governed only by the interaction of the LC flexopolarization with the photorefractive field (6) penetrating into the LC cell. To simplify the calculations, we shall also make the one elastic constant approximation $K_{11} = K_{22} = K_{33} = K$.

In the layers near the cell surfaces, $(-L/2, -l/2)$, $(l/2, L/2)$, we suppose a nematic ordering with absolutely rigid director anchoring and the director pretilt angles θ_{01} and θ_{02} at the cell surfaces $z = -L/2$ and $z = L/2$, respectively (Fig. 1). We introduce here the director in the form $\mathbf{n} = (\cos\vartheta(x,z), 0, \sin\vartheta(x,z))$, where $\vartheta(x,z)$ is a director angle with

the x-axis. Then the director can be parameterized as

$$\vartheta(x, z) = \theta_0(z) + [\theta(z)\exp(iqx) + c.c.]. \tag{10}$$

The free energy functional (8) is then minimized with respect to the angles $\theta_0(z)$ and $\theta(z)$. If $\vartheta(x, z)$ is small, we can linearise the resulting Euler-Lagrange equations in angles, yielding:

$$\frac{\partial^2\theta(z)}{\partial z^2} - q^2\theta(z) = \frac{e_1}{K}\frac{\partial E_{0x}}{\partial z} + iq\frac{e_3}{K}E_{0z} \tag{11}$$

$$\frac{\partial^2\theta_0}{\partial z^2} = 0 \tag{12}$$

In the central layer $(-l/2, l/2)$ the orientational ordering is cholesteric. In this region it is convenient to parameterize the director in the form $\mathbf{n} = (\cos\varphi(z)\sin\alpha(x, z), \sin\varphi(z)\sin\alpha(x, z), \cos\alpha(x, z))$, where $\alpha(x, z)$ is the director polar angle with the z-axis and $\varphi(z)$ is the director azimuth angle with respect to the x-axis. There is no experimental evidence that the cholesteric pitch changes in a photorefractive field [16], and so we suppose that photorefractive electric field does not influence the cholesteric pitch. We can then put $\varphi(z) = g \cdot (z + l/2)$. Putting $\alpha(x, z) = \frac{\pi}{2} - \tilde{\vartheta}(x, z)$ where $\tilde{\vartheta}(x, z)$ is the (small) director angle with the xy-plane and $\tilde{\vartheta}(x, z) = \tilde{\theta}_0(z) + [\tilde{\theta}(z)\exp(iqx) + c.c.]$ we obtain after minimization the free energy functional (8) the following equation for $\tilde{\theta}(z)$

$$\frac{\partial^2\tilde{\theta}(z)}{\partial z^2} - (q^2 + g^2)\tilde{\theta}(z) = -\frac{e_1 - e_3}{K}g\sin\varphi(z)E_{0x} + \left(\frac{e_1}{K}\frac{\partial E_{0x}}{\partial z} + iq\frac{e_3}{K}E_{0z}\right)\cos\varphi(z) \tag{13}$$

where we neglected influence of the small angle $\tilde{\theta}_0(z)$. Since a concentration of chiral molecules is small we can also neglect influence of chiral molecules on the director distribution induced by the director pretilt on the cell surfaces and approximately put $\tilde{\theta}_0(z) = \theta_0(z)$. Then solution of equation (12) for all area of the cell takes the form

$$\theta_0(z) = s + pz, \quad s = \frac{\theta_{01} + \theta_{02}}{2}, \quad p = \frac{\theta_{02} - \theta_{01}}{L}, \tag{14}$$

We then substitute expressions (7) for the electric field into eqs. (11), (13) using the boundary conditions at the surface of the cell:

$$\theta(-L/2) = 0, \quad \theta(L/2) = 0 \tag{15}$$

and the boundary conditions at the nematic-cholesteric boundary:

$$\theta(-l/2) = \tilde{\theta}(-l/2), \quad \left.\frac{\partial\theta}{\partial z}\right|_{z=-l/2} = \left.\frac{\partial\tilde{\theta}}{\partial z}\right|_{z=-l/2}, \quad \theta(l/2) = \tilde{\theta}(l/2),$$

$$\left.\frac{\partial\theta}{\partial z}\right|_{z=l/2} = \left.\frac{\partial\tilde{\theta}}{\partial z}\right|_{z=l/2}. \tag{16}$$

The solutions for the angles $\theta(z)$ and $\tilde{\theta}(z)$ are now:

a) in the layer $(-L/2, -l/2)$

$$\theta(z) \equiv \theta_1(z) = \frac{iE_{sc}(q)}{2q} D_1(z) m(-L/2),$$

$$D_1(z) = ie^{-\tilde{q}(L-l)/2} \left\{ \frac{f_1 + f_2 + \frac{q\tilde{q}r}{\tilde{q}^2 - q^2}[e^{(\tilde{q}-q)(L-l)/2} - 1]}{2sh[q(L-l)/2]} e^{q(z+L/2)} \right.$$

$$\left. - \frac{f_1 + f_2 + \frac{q\tilde{q}r}{\tilde{q}^2 - q^2}[e^{(\tilde{q}+q)(L-l)/2} - 1]}{2sh[q(L-l)/2]} e^{-q(z+L/2)} + \frac{q\tilde{q}re^{-\tilde{q}(z+l/2)}}{\tilde{q}^2 - q^2} \right\} \quad (17)$$

b) in the layer $(-l/2, l/2)$

$$\tilde{\theta}(z) = \frac{iE_{sc}(q)}{2q} [d_1(z)m(-L/2) + d_2(z)m(L/2)],$$

$$d_1(z) = ie^{-\tilde{q}(L-l)/2} \left[(f_1 + f_2 - f_3) e^{\sqrt{q^2+g^2}(z+l/2)} + (f_3 \cos\varphi + f_4 \sin\varphi) e^{-\tilde{q}(z+l/2)} \right]$$

$$d_2(z) = -ie^{-\tilde{q}(L-l)/2)} \left[(f_1 + (-1)^n f_2 - (-1)^n f_3) e^{\sqrt{q^2+g^2}(z-l/2)} \right.$$

$$\left. + (f_3 \cos\varphi - f_4 \sin\varphi) e^{\tilde{q}(z-l/2)} \right] \quad (18)$$

c) in the layer $(l/2, L/2)$

$$\theta(z) \equiv \theta_2(z) = \frac{iE_{sc}(q)}{2q} D_2(z) m(L/2),$$

$$D_2(z) = -ie^{-\tilde{q}(L-l)/2} \left\{ \frac{f_1 + (-1)^n f_2 + \frac{q\tilde{q}r}{\tilde{q}^2 - q^2}[e^{(\tilde{q}-q)(L-l)/2} - 1]}{2sh[q(L-l)/2]} e^{-q(z-L/2)} \right.$$

$$\left. - \frac{f_1 + (-1)^n f_2 + \frac{q\tilde{q}r}{\tilde{q}^2 - q^2}[e^{(\tilde{q}+q)(L-l)/2} - 1]}{2sh[q(L-l)/2]} e^{q(z-L/2)} + \frac{q\tilde{q}re^{\tilde{q}(z-l/2)}}{\tilde{q}^2 - q^2} \right\} \quad (19)$$

Where (ignoring some terms of order e^{-ql}):

$$f_1 = \frac{q\tilde{q}r}{\tilde{q}^2 - q^2} \frac{qch[q(L-l)/2] + \tilde{q}sh[q(L-l)/2] - qe^{\tilde{q}(L-l)/2}}{\sqrt{q^2+g^2}sh[q(L-l)/2] + qch[q(L-l)/2]},$$

$$f_2 = \frac{sh[q(L-l)/2][(\sqrt{q^2+g^2} - \tilde{q})f_3 + gf_4]}{\sqrt{q^2+g^2}sh[q(L-l)/2] + qch[q(L-l)/2]}, \quad (20)$$

$$f_3 = \frac{q\tilde{q}[r(\tilde{q}^2 - q^2 - 2g^2) + 2r_1g^2]}{(\tilde{q}^2 - q^2 - 2g^2)^2 + 4g^2\tilde{q}^2}, \quad f_4 = \frac{qg[r_1(\tilde{q}^2 - q^2 - 2g^2) - 2r\tilde{q}^2]}{(\tilde{q}^2 - q^2 - 2g^2)^2 + 4g^2\tilde{q}^2},$$

$$r = \frac{e_1 + e_3}{K}, \quad r_1 = \frac{e_1 - e_3}{K}. \quad (21)$$

Here n is a number of half-pitches along the length $l$of cholesteric layer in the cell.

4. Coupled Light Modes

4.1. Dielectric Tensor Profile

In the nematic layers, the LC dielectric tensor at an optical frequency $\varepsilon_{ij} = \varepsilon_\perp \delta_{ij} + \varepsilon_a n_i n_j$ can be written to second order in small director angle $\vartheta(x, z)$ as

$$\hat{\varepsilon} = \begin{pmatrix} \varepsilon_{||} - \varepsilon_a \vartheta^2(x,z) & 0 & \varepsilon_a \vartheta(x,z) \\ 0 & \varepsilon_\perp & 0 \\ \varepsilon_a \vartheta(x,z) & 0 & \varepsilon_\perp + \varepsilon_a \vartheta^2(x,z) \end{pmatrix}. \tag{22}$$

In the cholesteric layers, the analogous LC dielectric tensor can be expressed to second order in small director angle $\tilde{\theta}(x, z)$ as follows:

$$\hat{\varepsilon} = \begin{pmatrix} \varepsilon_\perp + \varepsilon_a \cos^2\varphi(1-\tilde{\theta}^2) & \frac{1}{2}\varepsilon_a \sin 2\varphi(1-\tilde{\theta}^2) & \varepsilon_a \tilde{\theta}\cos\varphi \\ \frac{1}{2}\varepsilon_a \sin 2\varphi(1-\tilde{\theta}^2) & \varepsilon_\perp + \varepsilon_a \sin^2\varphi(1-\tilde{\theta}^2) & \varepsilon_a \tilde{\theta}\sin\varphi \\ \varepsilon_a \tilde{\theta}\cos\varphi & \varepsilon_a \tilde{\theta}\sin\varphi & \varepsilon_\perp + \varepsilon_a \tilde{\theta}^2 \end{pmatrix}, \tag{23}$$

where in each case $\varepsilon_a = \varepsilon_\parallel - \varepsilon_\perp$, and $\varepsilon_|$,$\varepsilon_\perp$ are the principal values of the dielectric tensor. We now substitute $\vartheta(x, z) = \theta_0(z) + [\theta(z)\exp(iqx) + c.c.]$ into eq. (22) and $\tilde{\theta}(x, z) = \tilde{\theta}_0(z) + [\tilde{\theta}(z)\exp(iqx) + c.c.]$into eq. (23) and neglect small terms of second order in the angles $\theta(z)$ and $\tilde{\theta}(z)$. After some analysis, we obtain the following expression for the dielectric tensor:

$$\hat{\varepsilon}(x, z) = \hat{\varepsilon}_1(z) + \hat{\varepsilon}_2(z) + [\hat{\varepsilon}_3(z)\exp(iqx) + c.c.]. \tag{24}$$

The first term in eq. (24) corresponds to the LC with nematic ordering in layers $(-L/2, -l/2)$, $(L/2, l/2)$ and cholesteric ordering in the layer $(-l/2, l/2)$ at constant value of director angle with the xy-plane. The second term includes the inhomogeneity of the director distribution in the LC cell due to the boundary conditions at the cell planes. The third term describes the change of the dielectric tensor due to periodic modulation of the director by the dc photorefractive electric field with period $2\pi/q$. This is given by:

$$\begin{aligned} \hat{\varepsilon}_3(z) = \varepsilon_a \Bigg[& \begin{pmatrix} -2\theta_0(z) & 0 & 1 \\ 0 & 0 & 0 \\ 1 & 0 & 2\theta_0(z) \end{pmatrix} \cdot [\theta_1(z)\Delta(-z - l/2) + \theta_2(z)\Delta(z - l/2)] \\ & + \begin{pmatrix} -2\theta_0(z)\cos^2\varphi & -\theta_0(z)\sin 2\varphi & \cos\varphi \\ -\theta_0(z)\sin 2\varphi & -2\theta_0(z)\sin^2\varphi & \sin\varphi \\ \cos\varphi & \sin\varphi & 2\theta_0(z) \end{pmatrix} \\ & \times \tilde{\theta}(z)[1 - \Delta(-z - l/2) - \Delta(z - l/2)] \Bigg] \end{aligned} \tag{25}$$

where the function $\Delta(z)$ equals 1 when $z \geq 0$ and 0 when $z < 0$. Expressions for $\hat{\varepsilon}_1(z)$ and $\hat{\varepsilon}_2(z)$ are bulky and are omitted here.

4.2. Two Beam Light Propagation

The electric field of the light beams propagating in the LC cell can be written in the following form:

$$\mathbf{E}_{hv} = A_1(z)\mathbf{e}_1 \exp(i\mathbf{k}_1\cdot\mathbf{r} - i\omega t) + A_2(z)\mathbf{e}_2 \exp(i\mathbf{k}_2\cdot\mathbf{r} - i\omega t), \tag{26}$$

where (see Fig. 1) $\mathbf{e}_1 = (\cos\tilde{\alpha}_1, 0, -\sin\tilde{\alpha}_1)$, $\mathbf{e}_2 = (\cos\tilde{\alpha}_2, 0, \sin\tilde{\alpha}_2)$, $\mathbf{k}_1 = (k_1 \sin\alpha_1$ $0, k_1\cos\alpha_1)$, and $\mathbf{k}_2 = (-k_2\sin\alpha_2, 0, k_2\cos\alpha_2)$ are respectively the polarization and wave vectors of the two beams, and $k_1 = kn_1, k_2 = kn_2$, n_1, n_2 are refractive indices of LC for the first and second beams, respectively, and where $k = \omega/c$ is the (scalar) wave number of both beams in vacuum.

To estimate the rotation of the polarization of the incident light beams in the cholesteric layer within the cell [16] we use the standard expression for the rotation power per unit cell length [17]:

$$\frac{\psi}{L} = \frac{\pi}{16p_0}\left(\frac{n_e^2 - n_0^2}{n_e^2 + n_0^2}\right)^2 \frac{1}{(\lambda/p_0)^2\left[1 - (\lambda/p_0)^2\right]}, \tag{27}$$

This expression is valid for wavelengths λ greater than the cholesteric pitch p_0. The quantities n_0 and n_e are refraction indices for ordinary and extraordinary light waves, respectively. The values of parameters in experiments [16] were as follows: $\lambda = 0.532\,\mu$m, $p_0 = 0.45\,\mu$m, the refraction indices $n_0 = 1.527$, $n_e = 1.797$ for cholesteric mixture BL038/CB15 and $n_0 = 1.527$, $n_e = 1.744$ for cholesteric mixture TL205/CB15, with cell thickness $L = 5\,\mu$m.

Substituting these values into eq. (27) yields $\approx 0.1^c$. This rather small value is consistent with the experimental result that the transmitted optical polarization remains parallel to the polarization of light incident on the cell windows. We can thus conclude that in our case the light waves maintain their linear polarization even within that part of the LC cell which is specifically cholesteric.

The LC director is also subject to small deviations due to its pretilt on the cell surfaces and photorefractive field. In the simplest approximation, which we adopt here, we assume that these small director deviations also leave the beam polarizations and wave vectors unchanged, i.e they take values determined by supposing that the LC possesses dielectric tensor $\hat{\varepsilon}_1(z)$.

The light beam electric field satisfies the usual vector wave equation

$$[\nabla(\nabla\cdot) - \nabla^2]\mathbf{E}_{hv} - \frac{\omega^2}{c^2}\hat{\varepsilon}(x, z)\mathbf{E}_{hv} = 0. \tag{28}$$

We now substitute the electric field (26) and the dielectric tensor $\hat{\varepsilon}(x, z)$ (24) into formula (28). The leading order terms in this substitution cancel because each wave separately obeys the vector wave equation with dielectric tensor $\hat{\varepsilon}_1(z)$. The coupling between the waves takes place as a result of the corrections to the dielectric tensor $\hat{\varepsilon}_1(z)$[21]. The electric field magnitudes $A_1(z)$ and $A_2(z)$ then vary slowly across the cell. We follow a procedure analogous to that first outlined by Kogelnik [22] and used in our paper for the hybrid nematic cell [15]. Then, following paper [15], and after some complicated but not complex algebra, we obtain the set of coupled equations in the LC cell for the electric field magnitudes $A_1(z)$ and $A_2(z)$. Recalling beam 1 to be the signal and beam 2 to be the pump, we adopt the Undepleted Pump Approximation [21], for which the magnitude of the pump amplitude $|A_2| >> |A_1|$ and may be regarded as constant. In this case, the set of coupled

equations reduces to the following equation:

$$\frac{dA_1}{dz} = \frac{ik^2}{2k_{1z}}\mathbf{e}_1\hat{\varepsilon}_3\mathbf{e}_2 \exp(i\,\Delta k_z z)\,A_2, \tag{29}$$

where $\Delta k_z = k_{2z} - k_{1z}$ is proportional to small optical anisotropy of LC, ε_a, and with an accuracy to the small terms of the order of ε_a^2 the exponential multiplier in eq. (29) can be replaced by unity. We assume that the wave vectors of the light beams are symmetric with regard to the cell normal so as the angles α_1 and α_2 are equal and we can also put $\tilde{\alpha}_1 = \tilde{\alpha}_2$. The expression for the quantity $\mathbf{e}_1\hat{\varepsilon}_3\mathbf{e}_2$ in eq. (29) can be evaluated using eq. (25), finally yielding the following equation:

$$\begin{aligned}
&\frac{dA_1}{dz} = iS(z)A_2,\\
&S(z) = -\frac{i\varepsilon_a E_{sc}(q)}{2q}\frac{k^2}{k_{1z}}\theta_0(z)\{[D_1(z)\Delta(-z-l/2)m(-L/2) + D_2(z)\Delta(z-l/2)m(L/2)]\\
&\quad -[\cos^2\tilde{\alpha}_1\cos^2\varphi(z) + \sin^2\tilde{\alpha}_1][1-\Delta(-z-l/2)-\Delta(z-l/2)][d_1(z)m(-L/2)\\
&\quad + d_2(z)m(L/2)]\}
\end{aligned} \tag{30}$$

The solution to this equation has the following form:

$$A_1(z) = A_1(-L/2) + iA_2\int_{-L/2}^{z} S(z')dz' \tag{31}$$

4.3 Exponential Gain Coefficient

We now use eq. (31) to investigate energy exchange in the LC cell. The signal gain caused by the LC layer in hybrid cell is defined as

$$G = \frac{A_1(L/2)}{A_1(-L/2)}, \tag{32}$$

where from eq. (31)

$$A_1(L/2) = A_1(-L/2) + iA_2\int_{-L/2}^{L/2} S(z)dz \tag{33}$$

Now eq. (30) for $S(z)$ involves the quantities $m(\mp L/2)$. But in our case the pump amplitude $|A_2| \gg |A_1|$. Thus, we have $m(\mp L/2) \approx 2A_1(\mp L/2)\cos(2\delta)/A_2(\mp L/2)$. We use this expression in eq. (30) for $S(z)$, and then substitute the resulting formula for $S(z)$ into eq. (33). Combining eqs. (32) and (33) then yields:

$$\begin{aligned}
G = 1 + \frac{\varepsilon_a E_{sc}(q)}{q}\frac{k^2\cos(2\delta)}{k_{1z}}\Bigg\{&\int_{-L/2}^{-l/2}\theta_0(z)D_1(z)dz + \int_{-l/2}^{l/2}\theta_0(z)d_1(z)\\
&\times\left[\cos^2\tilde{\alpha}_1\cos^2\varphi(z) + \sin^2\tilde{\alpha}_1\right]dz + G[\int_{-l/2}^{l/2}\theta_0(z)d_2(z)[\cos^2\tilde{\alpha}_1\cos^2\varphi(z)\\
&+ \sin^2\tilde{\alpha}_1]dz + \int_{l/2}^{L/2}\theta_0(z)D_2(z)dz]\Bigg\}
\end{aligned} \tag{34}$$

Eq. (34) yields the following expression for G:

$$G = \frac{1 + a_1}{1 - a_2}, \tag{35}$$

where

$$a_1 = \frac{\varepsilon_a E_{sc}(q)}{q} \frac{k^2 \cos(2\delta)}{k_{1z}} \left\{ \int_{-L/2}^{-l/2} \theta_0(z) D_1(z) dz + \frac{1}{2} \int_{-l/2}^{l/2} \theta_0(z) d_1(z) [1 + \sin^2 \tilde{\alpha}_1 + \right.$$
$$\left. + \cos^2 \tilde{\alpha}_1 \cos 2\varphi(z)] dz \right\} \tag{36}$$

$$a_2 = \frac{\varepsilon_a E_{sc}(q)}{q} \frac{k^2 \cos(2\delta)}{k_{1z}} \left\{ \int_{l/2}^{L/2} \theta_0(z) D_2(z) dz + \frac{1}{2} \int_{-l/2}^{l/2} \theta_0(z) d_2(z) [1 + \sin^2 \tilde{\alpha}_1 \right.$$
$$\left. + \cos^2 \tilde{\alpha}_1 \cos 2\varphi(z)] dz \right\} \tag{37}$$

The exponential gain coefficient is now given by formula

$$\Gamma = \frac{1}{L} \ln \left| \frac{1 + a_1}{1 - a_2} \right| \tag{38}$$

Now substituting expressions (14) for $\theta_0(z)$ and (17)-(19) for $D_1(z)$,$D_2(z)$ and $d_1(z)$, $d_2(z)$ into (36), (37) we can perform the integration and arrive at

$$a_1 = \frac{i\varepsilon_a E_{sc}(q)}{4q} \frac{k^2 \cos(2\delta)}{k_{1z}} \left\{ - \frac{2rq[(2s - pl)e^{-\tilde{q}(L-l)/2} - 2\theta_{01}]}{\tilde{q}^2 - q^2} \right.$$
$$+ \frac{(2s - pl)e^{q(L-l)/2} - 2\theta_{01}]}{qsh[q(L-l)/2]} \left[(f_1 + f_2)e^{-\tilde{q}(L-l)/2} + rq\tilde{q} \frac{e^{-q(L-l)/2} - e^{-\tilde{q}(L-l)/2}}{\tilde{q}^2 - q^2} \right]$$
$$+ \frac{(2s - pl)e^{-q(L-l)/2} - 2\theta_{01}]}{qsh[q(L-l)/2]} \left[(f_1 + f_2)e^{-\tilde{q}(L-l)/2} + rq\tilde{q} \frac{e^{q(L-l)/2} - e^{-\tilde{q}(L-l)/2}}{\tilde{q}^2 - q^2} \right]$$
$$+ (2s - pl)e^{-\tilde{q}(L-l)/2}(1 + \sin^2 \tilde{\alpha}_1) \left(\frac{f_1 + f_2 - f_3}{\sqrt{q^2 + g^2}} + \frac{\tilde{q} f_3 + g f_4}{\tilde{q}^2 + g^2} \right)$$
$$+ (2s - pl)e^{-\tilde{q}(L-l)/2} \cos^2 \tilde{\alpha}_1) \left[\frac{\sqrt{q^2 + g^2}(f_1 + f_2 - f_3)}{q^2 + 5g^2} \right.$$
$$\left. \left. + \frac{1}{2} \left(\frac{\tilde{q} f_3 + 3g f_4}{\tilde{q}^2 + 9g^2} + \frac{\tilde{q} f_3 - g f_4}{\tilde{q}^2 + g^2} \right) \right] \right\} \tag{39}$$

$$a_2 = - \frac{i\varepsilon_a E_{sc}(q)}{4q} \frac{k^2 \cos(2\delta)}{k_{1z}} \left\{ - \frac{2rq[(2s + pl)e^{-\tilde{q}(L-l)/2} - 2\theta_{02}]}{\tilde{q}^2 - q^2} \right.$$
$$+ \frac{(2s + pl)e^{q(L-l)/2} - 2\theta_{02}]}{qsh[q(L-l)/2]} \left[(f_1 + (-1)^n f_2)e^{-\tilde{q}(L-l)/2} + rq\tilde{q} \frac{e^{-q(L-l)/2} - e^{-\tilde{q}(L-l)/2}}{\tilde{q}^2 - q^2} \right]$$
$$+ \frac{(2s + pl)e^{-q(L-l)/2} - 2\theta_{02}]}{qsh[q(L-l)/2]} \left[(f_1 + (-1)^n f_2)e^{-\tilde{q}(L-l)/2} + rq\tilde{q} \frac{e^{q(L-l)/2} - e^{-\tilde{q}(L-l)/2}}{\tilde{q}^2 - q^2} \right]$$
$$+ (2s + pl)e^{-\tilde{q}(L-l)/2}(1 + \sin^2 \tilde{\alpha}_1) \left[\frac{f_1 + (-1)^n f_2 - (-1)^n f_3}{\sqrt{q^2 + g^2}} + (-1)^n \frac{\tilde{q} f_3 + g f_4}{\tilde{q}^2 + g^2} \right]$$

$$+(2s+pl)e^{-\tilde{q}(L-l)/2}\cos^2\tilde{\alpha}_1)\left[\frac{\sqrt{q^2+g^2}(f_1+(-1)^n f_2-(-1)^n f_3)}{q^2+5g^2}\right.$$

$$\left.+\frac{(-1)^n}{2}\left(\frac{\tilde{q}f_3+3gf_4}{\tilde{q}^2+9g^2}+\frac{\tilde{q}f_3-gf_4}{\tilde{q}^2+g^2}\right)\right]\Bigg\} \tag{40}$$

Expressions (38)–(40) describe the exponential gain coefficient versus the parameters of the hybrid cholesteric cell.

5. Comparison with Experimental Data

We now compare our theoretical results with experimental data. We consider photorefractive hybrid cells with cholesteric mixtures obtained by doping the nematic LC TL205 or BL038 by cholesteric impurity CB15 [16]. We recall a key result from paper [15]. Here we showed that the director grating magnitude appears to depend nonlinearly on the photorefractive electric field magnitude $E_{sc}(q)$. The specific rule we obtained was that $E_{sc}(q)+\mu q^2 E_{sc}^3(q)$, with μ a fitting parameter.

The experiments [16] are considering a similar system, albeit chiral. In this spirit, we thus replace $E_{sc}(q)$ in formulas (39), (40) by $E_{sc}(q)+\mu q^2 E_{sc}^3(q)$. We also make the approximations that $\frac{k^2}{k_{1z}}\cos(2\delta)=\frac{\omega}{c}\frac{\cos(2\delta)}{n_1\cos\alpha_1}\approx 1.25\frac{\pi}{\lambda}$ and $\sin\tilde{\alpha}_1=\frac{q}{2k_1}\approx\frac{q}{3.2k}=\frac{q\lambda}{6.4\pi}$. In order to evaluate $E_{sc}(q)$ we have followed Cook et al. [23], who estimated that the ratio of the acceptor to donor impurity densities is very small, $N_d >> N_a$, and $N_a\approx 3.8\cdot 10^{21}\,m^{-3}$. The director pretilt angle at the LC cell substrates was approximately $12^0\approx 0.21^c$, yielding $\theta_{01}=-\theta_{02}=12^0\approx 0.21^{\mathrm{c}}$. The ratios of flexoelectric to elastic moduli $r=(e_1+e_3)/K$ and $r_1=(e_1-e_3)/K$ are not known for TL205/CB15 and BL038/CB15. But this ratio has been measured in other LC systems [24], and value of $1Cm^{-1}N^{-1}$ may be regarded as typical for absolute values of r and r_1. Putting $r=1Cm^{-1}N^{-1}$ we have three free parameters r_1,μ and thickness l of the LC layer with cholesteric ordering. These parameters are used to fit theoretical curves for exponential gain coefficient with experimental ones.

In Fig. 2(a) the gain coefficient Γ versus the grating spacing $\Lambda=2\pi/q$ is plotted for hybrid cell containing the LC mixture TL205/CB15. In Fig. 2(b) we show the analogous curve for the mixture BL038/CB15. Both cells have $L=5\,\mu$m. It turns out that the best fits for the theoretical curves (38) with the experimental data were obtained for fitting parameters which are almost equal in each case. The relevant values are $\mu=8\cdot 10^{-20}\,J^{-2}C^2m^4$, thickness of the layer with nematic ordering $(L-l)/2=0.03\ \mu$m and $r_1=-2.1Cm^{-1}N^{-1}$ for mixture TL205/CB15, $r_1=-2.2Cm^{-1}N^{-1}$ for mixture BL038/CB15.

6. Conclusions

We have developed a theoretical model to describe the experimentally observed energy gain of a weak signal beam interacting with a strong pump beam, incident on a diffraction grating in a hybrid cell filled with nematic LC doped by impurity chiral molecules. The grating is written on the director of the LC placed between two inorganic photorefractive windows. The space-charge field induced by interfering light beams in the photorefractive substrates penetrates into the LC and interacts with the LC director. In these systems the flexoelectric mechanism for electric field-director coupling is a more important than the LC static dielectric anisotropy coupling. The flexoelectric polarization in the bulk LC arises as a result of the initial director pretilt at the cell substrates. It is the principal physical

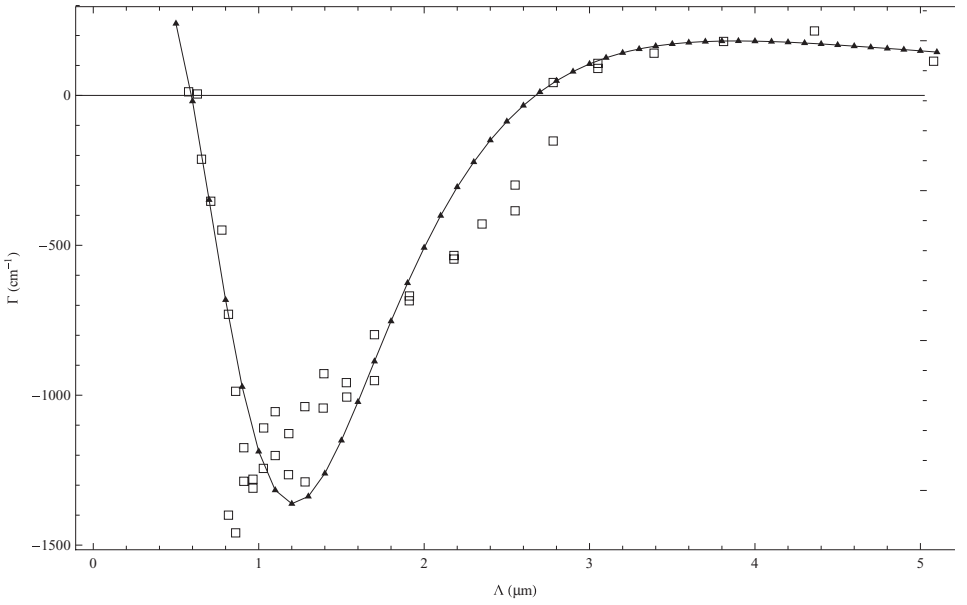

(a)

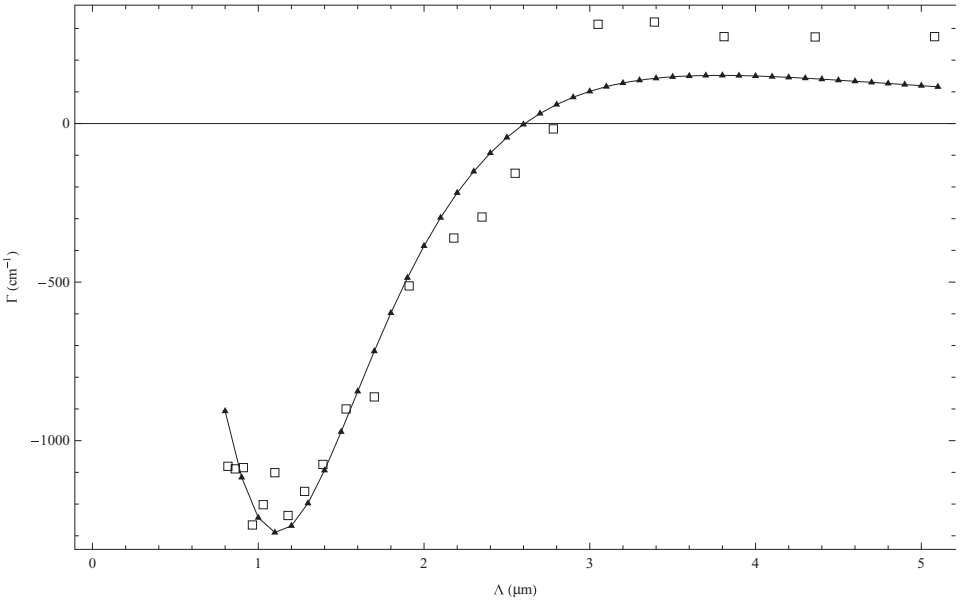

(b)

Figure 2. Gain coefficient Γ versus grating spacing Λ in hybrid cell filled by cholesteric LC mixture TL205/CB15 – (a) and BL038/CB15–(b). The cell thickness $L = 5\,\mu m$. Experimental data–boxes.

mechanism governing the magnitude of the director grating and hence of the two-beam coupling.

For hybrid cells filled with cholesteric mixtures TL205/CB15 and BL038/CB15, we find that a fit between the experiments and theory for the gain coefficient in two-beam energy exchange can be achieved. We believe that the fit provides good evidence that the key physics of these systems has been correctly identified. However the fit requires not only the inclusion of a non-linear contribution to the magnitude of the director grating as a function of photorefractive electric field, but also the assumption that close to LC cell surfaces the mixture behaves essentially as a nematic.

The non-linear contribution of the photorefractive field to the magnitude of the director grating has been included phenomenologically. However, it is of the same form and of the same order of magnitude as that successfully used in a previous theory on analogous nematic systems. Although there is no independent verification of this hypothesis, the fact that the same phenomenon occurs in three different (albeit similar) systems is good circumstantial evidence that the hypothesis is at least on the right lines. Some semi-empirical calculations as to the origin of the non-linear field leakage were included in ref [15], but they are not yet conclusive. Further microscopic calculations are required to confirm that the non-linear field leakage is occurring in the way that we suppose, as well as independent experiments.

The second hypothesis should be regarded at this stage as a plausible working hypothesis. Clearly some confirmation is achieved by the very fact that a fit is possible. The nematic region is rather thin as compared to the thickness of the LC layer as a whole. In fact we should expect a smooth variation of both the degree of chirality and of the chiral component. It would be useful to have both microscopic free energy calculations showing that this assumption is plausible, and also independent experimental results which show that the chiral component segregation is really occurring. Both elements of this program are currently under active consideration for future research.

Acknowledgments

This work has been partially supported by EOARD Grant 078001(V.Y.R. and I.P.P.). Some of the work was carried out in the Department of Physics at the University of Maribor, Slovenia. T.J. Sluckin thanks the Department of Education of the Republic of Slovenia for a visiting professorship enabling this visit.

References

[1] Rudenko, E. V., & Sukhov, A. V. (1994). *JETP Lett.*, *59*, 142.
[2] Rudenko, E. V., & Sukhov, A. V. (1994). *JETP*, *78*, 875.
[3] Khoo, I. C., Li, H., & Liang, Y. (1994). *Opt. Lett.*, *19*, 1723.
[4] Brignon, A., Bongrand, I., Loiseaux, B., & Huignard, J. P. (1997). *Opt. Lett.*, *22*, 1855.
[5] Kajzar, F., Bartkiewicz, S., & Miniewicz, A. (1999). *Appl. Phys. Lett.*, *74*, 2924.
[6] Bartkiewicz, S., Matczyszyn, K., Miniewicz, A., & Kajzar, F. (2001). *Opt. Commun.*, *187*, 257.
[7] Wiederrecht, G. P., Yoon, B. A., & Wasielewski, M. R. (1995). *Science*, *270*, 1794.
[8] Khoo, I. C., Guenther, B. D., Wood, M. V., Chen, P., & Shih, M.-Y. (1997). *Opt. Lett.*, *22*, 1229.
[9] Ono, H., & Kawatsuki, N. (1999). *J. Appl. Phys.*, *85*, 2482.
[10] Cook, G., Carns, J. L., Saleh, M. A., & Evans, D. R. (2006). *Mol. Cryst. Liq. Cryst.*, *453*, 141.
[11] Sutherland, R. L., Cook, G., & Evans, D. R. (2006). *Opt. Express*, *14*, 5365.
[12] Evans, D. R., & Cook, G. (2007). *J. Nonlinear Opt. Phys. Mater.*, *16*, 271.
[13] Tabiryan, N. V., & Umeton, C. (1998). *J. Opt. Soc. Am. B*, *15*, 1912.
[14] Jones, D. C., & Cook, G. (2004). *Opt. Commun.*, *232*, 399.

[15] Reshetnyak, V. Yu., Pinkevych, I. P., Cook, G., Evans, D. R., & Sluckin, T. J. (2010). *Phys. Rev. E*, *81*, 031705–(1-15).
[16] Cook, G., Beckel, E., Reshetnyak, V. Yu., Saleh, M. A., & Evans, D. R. (2007). In: *Controlling Light with Light: Photorefractive Effects, Photosensitivity, Fiber Gratings, Photonic Materials and More: OSA Technical Digest (CD) [Photorefractive Effects, Photosensitivity, Fiber Gratings, Photonic Materials and More (PR) Squaw Creek, California October 2007]*, Optical Society of America: Washington, DC.
[17] See e.g. de Gennes, P. G., & Prost, J. (1993). *The Physics of Liquid Crystals*, Clarendon Press: Oxford, Ch 6.
[18] Pinkevich, I. P., Reshetnyak, V. Yu., & Lednei, M. F. (1992). *Ukr. Phys. J.*, *37*, 218.
[19] Kralj, S., & Sluckin, T. J. (1995). *Liq. Cryst.*, *18*, 887.
[20] Schmidke, J., & Coles, H. J. (2009). *Phys. Rev E.*, *80*, 011702.
[21] Yeh, P. (1993). *Introduction to Photorefractive Nonlinear Optics*, Wiley.
[22] Kogelnik, H. (1969). *Bell Syst. Tech. J.*, *48*, 2909.
[23] Cook, G., Carns, J. L., Saleh, M. A., & Evans, D. R. (2006). *Mol. Cryst. Liq. Cryst.*, *453*, 141.
[24] Edwards, E. G., Brown, C. V., Kriezis, E. E., & Elston, S. J. (2003). *Mol. Cryst. Liq. Cryst.*, *400*, 13.